JOURNAL OF GUIDANCE, CONTROL, AND DYNAMICS
Vol. 39, No. 12, December 2016

Check for updates

Solar-Sail Trajectory Design for a Multiple Near-Earth-Asteroid Rendezvous Mission

Alessandro Peloni* and Matteo Ceriotti†
University of Glasgow, Glasgow, Scotland G12 8QQ, United Kingdom
and
Bernd Dachwald‡
FH Aachen University of Applied Sciences, 52064 Aachen, Germany

DOI: 10.2514/1.G000470

The scientific interest for near-Earth asteroids as well as the interest in potentially hazardous asteroids from the perspective of planetary defense led the space community to focus on near-Earth asteroid mission studies. A multiple near-Earth asteroid rendezvous mission with close-up observations of several objects can help to improve the characterization of these asteroids. This work explores the design of a solar-sail spacecraft for such a mission, focusing on the search of possible sequences of encounters and the trajectory optimization. This is done in two sequential steps: a sequence search by means of a simplified trajectory model and a set of heuristic rules based on astrodynamics, and a subsequent optimization phase. A shape-based approach for solar sailing has been developed and is used for the first phase. The effectiveness of the proposed approach is demonstrated through a fully optimized multiple near-Earth asteroid rendezvous mission. The results show that it is possible to visit five near-Earth asteroids within 10 years with near-term solar-sail technology.

Downloaded by UCHU KOKU KENKYU KAIHATSU KIKO on March 1, 2021 | http://arc.aiaa.org | DOI: 10.2514/1.G000470

Nomenclature

A	=	sail area, m^2
$\boldsymbol{A}$	=	matrix of the dynamics
$\boldsymbol{a}$	=	solar-sail acceleration, mm/s^2
a	=	semimajor axis, astronomical unit
a_c	=	solar-sail characteristic acceleration, mm/s^2
$\boldsymbol{b}$	=	auxiliary vector of the dynamics
e	=	eccentricity
$\hat{\boldsymbol{e}}$	=	eccentricity unit vector
f, g	=	in-plane modified equinoctial elements
H	=	asteroid absolute magnitude
$\hat{\boldsymbol{h}}$	=	orbital angular momentum unit vector
i	=	inclination, deg
J	=	objective function for the genetic algorithm
j, k	=	out-of-plane modified equinoctial elements
L	=	true longitude, rad
m	=	total sailcraft mass, kg
$\hat{\boldsymbol{N}}$	=	unit vector normal to the sail plane
P_q^n	=	number of q permutations of n objects
p	=	semilatus rectum, astronomical unit
$\boldsymbol{r}$	=	sun–spacecraft position vector ($r := \|\boldsymbol{r}\|$), astronomical unit
$\hat{\boldsymbol{r}}$	=	sun–spacecraft unit vector
$\ddot{\boldsymbol{r}}$	=	acceleration
$r_\oplus$	=	mean sun–Earth distance, 1 astronomical unit
t	=	time, s
t_0	=	launch date
$\boldsymbol{u}$	=	control vector
$\boldsymbol{v}$	=	velocity vector
W_1, W_2	=	weighting factors
$\boldsymbol{x}$	=	state vector in modified equinoctial elements
$\boldsymbol{x}^{\text{kep}}$	=	state vector in Keplerian elements
α	=	sail cone angle, deg
Δv	=	velocity increment, km/s
δ	=	sail clock angle, deg
$\delta\varpi$	=	longitude of pericenter variation, rad
ζ	=	angle between two consecutive sailcraft attitudes, deg
$\hat{\boldsymbol{\vartheta}}$	=	in-plane transversal unit vector
θ	=	angle between angular momenta of two orbits, deg
λ_p	=	shaping parameter related to semilatus rectum, astronomical unit
λ_{fg}	=	shaping parameter related to in-plane modified equinoctial elements
μ	=	gravitational parameter of the central body, 1.3271×10^{11} km^3/s^2
ν	=	true anomaly, rad
τ	=	attitude-control torque, N · m
φ_p	=	phasing parameter related to semilatus rectum, rad
φ_{fg}	=	phasing parameter related to in-plane modified equinoctial elements, rad
Ω	=	right ascension of the ascending node, rad
ω	=	argument of pericenter, rad
ϖ	=	longitude of pericenter, rad

Subscripts

F	=	value dependent on boundary conditions at final time
f	=	final value
I	=	value dependent on boundary conditions at initial time
max	=	maximum
min	=	minimum
0	=	initial value

Superscripts

d	=	desired value
p	=	value after propagation
T	=	transpose
$*$	=	optimal value of the variable
$\cdot$	=	time derivative

Received 11 February 2016; revision received 27 June 2016; accepted for publication 11 July 2016; published online 7 September 2016. Copyright © 2016 by Alessandro Peloni, Matteo Ceriotti, and Bernd Dachwald. Published by the American Institute of Aeronautics and Astronautics, Inc., with permission. Copies of this paper may be made for personal and internal use, on condition that the copier pay the per-copy fee to the Copyright Clearance Center (CCC). All requests for copying and permission to reprint should be submitted to CCC at www.copyright.com; employ the ISSN 0731-5090 (print) or 1533-3884 (online) to initiate your request.

*Ph.D. Candidate, School of Engineering, James Watt (South) Building; a.peloni.1@research.gla.ac.uk. Student Member AIAA.

†Lecturer, School of Engineering, James Watt (South) Building; Matteo.Ceriotti@glasgow.ac.uk. Member AIAA.

‡Professor, Faculty of Aerospace Engineering; dachwald@fh-aachen.de.

Downloaded by UCHU KOKU KENKYU KAIHATSU KIKO on March 1, 2021 | http://arc.aiaa.org | DOI: 10.2514/1.G000470

I. Introduction

SOLAR sailing is an attractive way to perform interplanetary transfers that would otherwise be very challenging, even for high-I_{sp} low-thrust propulsion systems. Because a solar sail is propelled only by sunlight, it is a propellantless low-thrust propulsion system. This makes solar sailing an appealing option for performing high-Δv interplanetary missions [1], as well as non-Keplerian orbits [2], which require continuous thrusting [3]. Moreover, because of the unlimited Δv available, a solar-sail mission could cope with contingencies and enable a change of the target bodies, even after launch. This is particularly interesting for small-body missions, because dozens of new objects are discovered on a daily basis. Because of this advantage, several studies have been carried out on the application of solar sails for interplanetary missions, from an orbital dynamics point of view, as well as from a structural one [4,5].

Great effort has been dedicated to the study of near-Earth asteroids (NEAs) because of their importance from a scientific, technological, and planetary-defense point of view. Regarding the latter, several NEAs pose a potential threat to our planet and are indeed classified as potentially hazardous asteroids (PHAs). A multiple-NEA rendezvous mission with close-up observations of several objects can help the scientific community to improve the knowledge about the diversity of these objects and to support any future mitigation act. Furthermore, a multiple-target mission is preferable to a simple single-rendezvous mission because of the reduced cost of each observation and the intrinsic lack of knowledge that makes the choice of a single target difficult. Such a mission, however, is challenging from a mission planning point of view because of the large number of objects and the huge number of different ordered sequences of NEAs that can be chosen to visit. This is first a combinatorial problem with more than a billion possible sequences with only three consecutive encounters. Moreover, because no closed-form solutions exist for low-thrust trajectories, a trajectory optimization problem must be solved numerically for each leg of the multiple rendezvous to test the feasibility of the proposed sequence with the propulsion system used. Several approaches have been presented in the literature to deal with low-thrust trajectory optimization problems [6]: These are mainly categorized into direct, indirect, and evolutionary methods. In addition, shape-based approaches have been developed to have a fast trajectory solution for a preliminary mission design [7,8].

Several methodologies for low-thrust mission design have been studied, for example, by using shape-based methods [7,9] or by dividing the trajectory into segments [10] or finite elements [11]. To compare high-thrust with low-thrust mission design, Izzo [12] discussed a way to solve two-dimensional versions of Lambert's problem with Petropoulos and Longusky's shape-based function [13]. The astrodynamics community has shown much interest in asteroid-related trajectory optimization problems and mission design, such that six out of eight problems of the Global Trajectory Optimisation Competition[§] (GTOC) deal with asteroid-related missions. In the fourth GTOC problem, for example, the challenge was to visit the largest possible number of NEAs with a low-thrust spacecraft within a given total mission duration.[¶] In the majority of the solutions proposed,[**] the problem was divided into two main steps: first looking for a sequence of encounters by means of impulsive thrusts, then converting the high-thrust solutions found into low-thrust trajectories.

With respect to solar sails, most of the literature focuses on single-phase problems, whereas two of the few works on multiphase solar-sail trajectories are the ENEAS+ mission studies [1] and the Gossamer Roadmap technology reference study presented by Dachwald et al. [14]. In both cases, a systematic assessment of all possible asteroids to be visited in a multiple rendezvous mission has not been carried out. The sequences of encounters have been in fact decided a priori and the trajectory-optimization phase is mainly discussed. Bando and Yamakawa [15] describe an NEA survey mission using solar-sailing technology. However, this study is focused on flybys only and two-dimensional dynamics are taken into account for the solar-sail motion. In the same paper, an inverse solar-sail trajectory problem is described, generalizing what is presented by McInnes [16] by taking into account a less-performing solar sail. The method consists of deriving an analytic sail steering law that allows a solar-sail transfer between two planar circular heliocentric orbits with the same radii but different angular velocities.

This paper presents for the first time a shape-based approach used to approximate solar-sail trajectories, combined with a method to select sequences of encounters for a multiple-NEA rendezvous mission through solar sailing. The study carried out in this paper is divided into three main steps: first, a new set of shaping functions is investigated for the coplanar solar-sail scenario. Then, a search-and-prune algorithm is used to find sequences of target bodies by means of the shape-based trajectory model developed. Last, the sequences that best fit the mission requirements are converted into solar-sail trajectories using an optimization based on a Radau pseudospectral method [17–19].

The paper is organized as follows: In Sec. II, the shape-based approach developed for solar sailing is detailed. Sections III and IV describe the sequence-search algorithm and the optimization process used to test the sequences found, respectively. In Sec. V, the results of the method described are shown, and Sec. VI presents our conclusions.

II. Shape-Based Approach for Solar Sailing

A. Solar-Sailing Shape Description

In general, low-thrust trajectories have no analytical closed-form solutions, and so a numerical optimization strategy is generally used in trajectory design. A first-guess solution is a fast and low-accuracy solution, which is generally used in a preliminary phase of the mission design. An initial guess is also needed if the chosen optimization method uses a direct transcription [20].

First proposed by Petropoulos and Longusky in 2004 [13], the shape-based approach describes the shape of the trajectory with an appropriate set of mathematical expressions, such that $\boldsymbol{r}(t)$ is given. In the two-body problem approximation, the acceleration required to follow a specified trajectory is then retrieved by

$$\boldsymbol{a} = \ddot{\boldsymbol{r}} + \mu \frac{\boldsymbol{r}}{r^3} \tag{1}$$

The advantage of this method is that the trajectory is defined analytically and so no optimization is needed, although there is no

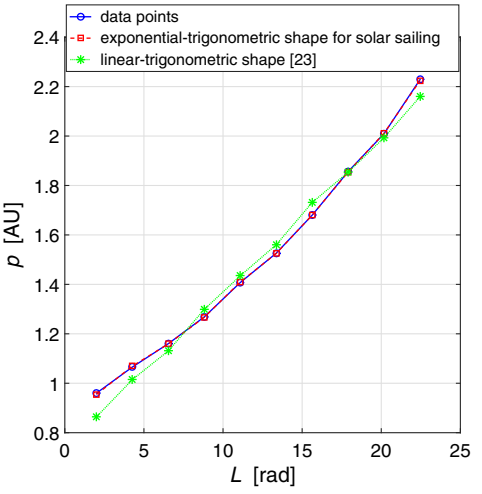

Fig. 1 Semilatus rectum over true longitude.

[§]Data available online at http://sophia.estec.esa.int/gtoc_portal/ [retrieved 25 August 2015].

[¶]Bertrand, R., Epenoy, R., and Meyssignac, B., "Problem Description for the 4th Global Trajectory Optimisation Competition," 2009, http://www .esa.int/gsp/ACT/doc/MAD/ACT-RPT-MAD-GTOC4-problem_stmt. pdf [retrieved 21 August 2014].

**Bertrand, R., Epenoy, R., and Meyssignac, B., "Final Results of the 4th Global Trajectory Optimisation Competition," 2009, http://mech.math. msu.su/~iliagri/gtoc4/gtoc4_final_results.pdf [retrieved 24 April 2014].

Table 1 Statistical values of the fits for p, f, and g

Statistical values	Shape-based approach	p	f	g
SSE	Shape in [23]	1.489	0.3972	0.3655
	Solar-sailing shape	4×10^{-3}	4.5×10^{-4}	3.9×10^{-4}
ARS	Shape in [23]	0.989	0.6991	0.6679
	Solar-sailing shape	1.0000	0.9997	0.9996

guarantee that the solution found is optimal. Furthermore, the shape can be chosen such that the thrust profile can be obtained analytically. On the other hand, there are no explicit constraints that limit the required acceleration, which can then result to be well above the thrusting capabilities.

Different shapes have been proposed to date [13,21–23] and all of them are studied for low-thrust problems with the simplification of tangential thrust. Unlike in thruster-based systems, however, the acceleration given by a solar sail is constrained in direction, with no thrust available toward the sun and neither entirely in the transversal direction. Moreover, a correlation between thrust direction and thrust magnitude characterizes the dynamics of a solar sail. The acceleration given by a perfectly reflecting solar sail at the distance r from the sun can be expressed as

$$\boldsymbol{a} = a_c \left(\frac{r_\oplus}{r}\right)^2 \cos^2\alpha \hat{\boldsymbol{N}} \tag{2}$$

In the orbital reference frame $\{\hat{\boldsymbol{r}}, \hat{\boldsymbol{\vartheta}}, \hat{\boldsymbol{h}}\}$, $\hat{\boldsymbol{N}}$ can be expressed by means of the cone angle α and the clock angle δ, so that $\hat{\boldsymbol{N}} = [\cos\alpha \quad \sin\alpha\cos\delta \quad \sin\alpha\sin\delta]^T$. The term a_c in Eq. (2) is the so-called characteristic acceleration and it represents the acceleration given by the solar sail facing the sun (i.e., $\alpha = 0$) at Earth distance [i.e., $r_\oplus = 1$ astronomical unit (AU)].

Because of the different constraints on the thrust, a set of shaping functions for solar sailing has been investigated with the use of the modified equinoctial elements $\boldsymbol{x} = [p, f, g, j, k, L]^T$ [24]. A coplanar approximation has been considered, so that the out-of-plane elements j and k do not have to be considered.

To find a shape of the trajectory that can be achieved with the solar-sail thrust constraints, several shaping functions have been investigated over two test cases. Each one of the three in-plane modified equinoctial elements $\{p, f, g\}$ is studied separately as function of the true longitude L. The three shaping functions found are compared with the linear-trigonometric shape presented by De Pascale and Vasile [23]. For each element, the MATLAB Curve Fitting toolbox [25] has been used to find the function that best fits the data points. Three parameters have been taken into account to determine the quality of the fit: 1) how much the fitting curve actually overlaps the data in the plot, 2) the sum of squares due to error (SSE), and 3) the adjusted R-square (ARS). To be a good fit, the value of SSE must be as close to zero as possible, whereas the value of ARS must be as close to one as possible.

In the first test case, the heliocentric trajectory of a sail with a constant cone angle of $\alpha = 35$ deg is numerically propagated for seven years, starting from the initial orbit stated in Eq. (3):

$$\boldsymbol{x}_0^{\text{kep}} = [\, r_\oplus \quad 0.2 \quad 0 \quad 0 \quad 0 \quad 2 \text{ rad}\,]^T \tag{3}$$

in which $\boldsymbol{x}^{\text{kep}} = [a, e, i, \Omega, \omega, \nu]^T$ is the tuple of (conventional) Keplerian elements. The sailcraft considered in this test case has a characteristic acceleration of $a_c = 0.3$ mm/s^2.

The shaping function that best describes the evolution of the semilatus rectum p by means of solar sailing is an exponential-trigonometric shape in the following form:

$$p = p_I \exp[p_F(L - L_0)] + \lambda_p \sin(L + \varphi_p) \tag{4}$$

in which p_I and p_F depend on the initial and final conditions, and λ_p and φ_p are, respectively, the shaping and phasing parameters related to the semilatus rectum. Figure 1 shows the fit of the semilatus rectum p against the true longitude L through both the linear-trigonometric shape presented in [23] and the exponential-trigonometric shape of Eq. (4). It can be seen that the linear-trigonometric shape (dotted line with asterisks) does not overlap exactly the data (solid line with circles). On the other hand, the exponential-trigonometric shape (dashed line with squares) fits well with the data points. The quantitative parameters SSE and ARS for both the shaping functions are shown in Table 1.

The functions that best describe the evolution of the two in-plane elements f and g by means of solar sailing are linear-trigonometric shapes in the following form:

$$\begin{aligned} f &= f_I + f_F(L - L_0) + \lambda_{fg} \sin(L + \varphi_{fg}) \\ g &= g_I + g_F(L - L_0) - \lambda_{fg} \cos(L + \varphi_{fg}) \end{aligned} \tag{5}$$

in which λ_{fg} and φ_{fg} are the shaping and phasing parameters related to the in-plane elements f and g.

Table 1 shows the statistical values used to measure the quality of the fit, whereas Fig. 2 shows the fits of the in-plane elements f and g through the linear-trigonometric shapes developed for solar sailing and the ones from [23]. As for the semilatus rectum, both the statistical values of the fits and the plot of the fitting curves against the data points show how the new set of shaping functions for solar sailing better describes the solar-sail trajectory than the linear-trigonometric functions presented in [23].

For the second test case, an Earth–Mars coplanar orbit transfer through a solar sail with characteristic acceleration of $a_c = 1$ mm/s^2 is considered. The reference orbit is computed via an indirect optimization approach, as in Mengali and Quarta [26]. The statistical values of the fits are shown in Table 2, whereas Fig. 3 shows the fits of

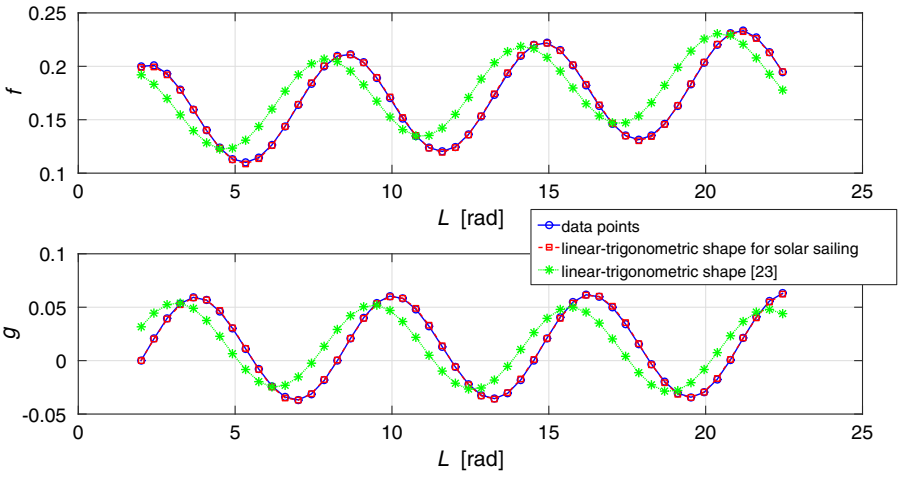

Fig. 2 In-plane elements f and g over true longitude.

Downloaded by UCHU KOKU KENKYU KAIHATSU KIKO on March 1, 2021 | http://arc.aiaa.org | DOI: 10.2514/1.G000470

Table 2 Earth–Mars coplanar orbit transfer[a]

Statistical values	Shape-based approach	p	f	g
SSE	Shape in [23]	1.2×10^{-1}	9.5×10^{-2}	3.3×10^{-1}
	Solar-sailing shape	8.9×10^{-3}	1.7×10^{-2}	2.7×10^{-3}
ARS	Shape in [23]	0.9880	0.9615	0.6512
	Solar-sailing shape	0.9991	0.9928	0.9972

[a]Statistical values of the fits for p, f, and g.

the in-plane modified equinoctial elements over true longitude. From this test case, as well as from the previous one with a constant thrust, it is clear how the new set of shaping functions better describes a solar-sail trajectory.

B. Use of Shape-Based Approach to Find First-Guess Trajectory

As shown in Eqs. (4) and (5), given an initial and final state, the trajectory is defined with the four free parameters $[\lambda_p, \lambda_{fg}, \varphi_p, \varphi_{fg}]$. The acceleration $\boldsymbol{a}$ needed to follow the shape of the trajectory defined by the shaping and phasing parameters is then analytically retrieved through Eq. (1). The control history is changed by tuning these parameters such that the constraints on the achievable thrust [Eq. (2)] are satisfied. To do so, the free parameters, as well as the time of flight and the number of complete revolutions, have been searched with the MATLAB built-in genetic algorithm (GA).

Because the acceleration needed to follow the shaped trajectory is only retrieved a posteriori, a set of nonlinear constraints is implemented within the GA to force the shaped trajectory to be as close as possible to a solar-sail trajectory. The nonlinear constraints are set so that 1) the magnitude of the acceleration is the one that the selected sailcraft can provide, 2) the acceleration is never directed toward the sun, and 3) the time of flight is consistent with the time resulting from the integration of the variation of the true longitude. This last constraint is necessary to make the solution physical, because it is the only link between the time of flight and the shaped trajectory, as discussed in [9,23].

The objective function of the GA can be changed according to the application. In this paper, two different objective functions have been used. When used within the sequence-search phase, the shaping functions are found by minimizing the time of flight. This objective function has been chosen because it guarantees a fast optimization, because the time of flight is one of the optimization variables. This way, the evaluation of the objective function by the GA is very fast, so that only the evaluation of the function of the constraints requires computational time. However, because the relation between magnitude and direction of the acceleration is not explicitly constrained, the trajectory propagated by using the control angle derived from the shaping functions can differ with respect to the real one. For this reason, when used as an initial-guess solution for the local optimization, a different objective function is used. The objective function J is chosen to minimize the error between the final state due to propagation and the final desired state. This objective function is shown in Eq. (6), where $W_1 = 1000$ and $W_2 = 10$ are two dimensionless weighting factors. These factors have been found after a trial-and-error process and have been chosen with the purpose of weighting the error in position more than the one in velocity. Despite weights different than those ones

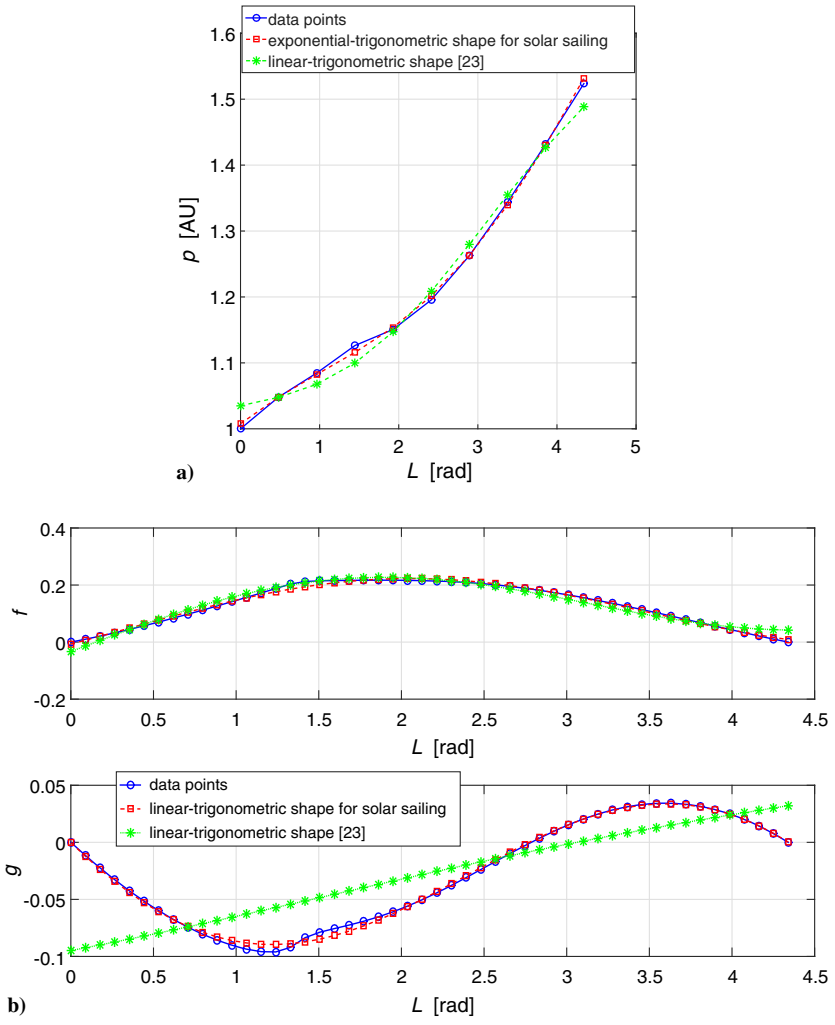

Fig. 3 Earth–Mars coplanar orbit transfer: a) semilatus rectum and b) in-plane elements f and g over true longitude.

Downloaded by UCHU KOKU KENKYU KAIHATSU KIKO on March 1, 2021 | http://arc.aiaa.org | DOI: 10.2514/1.G000470

proposed would produce different solutions, the methodology would not change, and the final choice on the weights is therefore ultimately for the mission analyst. Moreover, position and velocity are scaled so that $r_\oplus = 1$ and $\mu = 1$:

$$J = W_1 \cdot \|\boldsymbol{r}_f^p - \boldsymbol{r}_f^d\| + W_2 \cdot \|\boldsymbol{v}_f^p - \boldsymbol{v}_f^d\| \tag{6}$$

III. Sequence Search

Finding a sequence of NEAs to be visited is first a combinatorial problem because of the large amount of objects and the huge number of possible permutations between them, as pointed out in Sec. III.A. Furthermore, for each object, an optimization problem must be solved to assess the existence of a solar-sail trajectory. For the preceding reasons, a reduced database of NEAs has been used for the sequence search, as explained in detail in Sec. III.A. Moreover, for each leg of the sequence, a local pruning on the reduced database has been carried out to further reduce the amount of objects to test, as detailed in Sec. III.C.

In the following sections, a description of the asteroid selection for the reduced database and a detailed explanation of the sequence-search algorithm are given.

A. Asteroid Database Selection

The choice of target asteroids to be visited in a mission is difficult because it shall consider composition, scientific interest, orbital dynamics, and available launch windows. There are 12,840 NEAs discovered to date[††] and this number is increasing rapidly. All those objects with an Earth minimum orbit intersection distance (EMOID) $\leq$0.05 AU and an absolute magnitude $H \leq 22$ (i.e., diameter $\geq 110 - 240$ m, depending on the albedo[‡‡]) are classified as PHAs. Because there seem to be no clear common priorities on the selection of NEAs in the scientific community, the problem of finding a sequence of encounters is first a combinatorial problem, with more than a billion possible combinations with permutations of only three objects. To reduce this huge amount of possible combinations, a second classification method can be considered, taking into account those objects that are part of the Near-Earth Object Human Space Flight Accessible Target Study (NHATS) [27]. The objects in this list are those for which a low-thrust return mission can be found, as constrained by the following mission parameters: total Δv required, total mission duration, stay time at the object, and launch date interval. Because the mission parameters for the trajectory computation can be set in several different ways, the list of NHATS asteroids is not univocally defined.

To have a more usable and interesting database, only PHAs and NHATS asteroids are taken into account in the current work, leading to a reduced database of 1801 objects, 1597 of which are PHAs. The criteria used to select the NHATS database are the following:

$$\text{NHATS criteria:} \begin{cases} \text{total } \Delta v \text{ required} \leq 8 \text{ km/s} \\ \text{total mission duration} \leq 450 \text{ days} \\ \text{stay time at the object} \geq 8 \text{ days} \\ \text{launch: 2015–2040} \\ H \leq 26 \text{ magnitude} \\ \text{OCC} \leq 7 \end{cases} \tag{7}$$

in which OCC is the orbit condition code of an NEA's orbit, which refers to the orbit determination accuracy. For a complete explanation of the preceding criteria, the interested reader is referred to the Jet Propulsion Laboratory/NASA NHATS website.[§§]

[††]Data available online at http://neo.jpl.nasa.gov/cgi-bin/neo_elem [retrieved 08 August 2015].

[‡‡]Data available online at http://www.minorplanetcenter.net/iau/lists/Sizes.html [retrieved 25 August 2015].

[§§]Data available online at http://neo.jpl.nasa.gov/nhats/ [retrieved 08 August 2015].

Table 3 Number of q permutations of n objects within complete and reduced databases

Database	n	$q = 3$	$q = 4$	$q = 5$
Complete database	12,840	2.1×10^{12}	2.7×10^{16}	3.5×10^{20}
Reduced database	1,801	5.8×10^{9}	1.0×10^{13}	1.9×10^{16}

An order of magnitude for the complexity of the problem of finding a sequence of encounters can be given by considering the total number of possible sequences of $q = 3$, 4, and 5 objects without repetition, both from the original and the reduced database. The number of these q permutations of n objects P_q^n (Table 3) is given by

$$P_q^n = \frac{n!}{(n-q)!} \tag{8}$$

B. Sequence-Search Algorithm

The sequence-search algorithm works as follows (Fig. 4): The whole database is locally pruned by means of heuristic rules based on astrodynamics (details in Sec. III.C) and by taking into account that the sequence starts at Earth at a fixed time t_0. This pruning allows the algorithm to take into account fewer objects at a time, avoiding spending time on those objects that would be difficult to reach. Approximated solar-sail trajectories are found by means of the shape-based approach described in Sec. II. For all the trajectories found, the arrival NEAs are kept and considered as starting objects for the next iteration of the algorithm. Next, once the objects in the current pruned list have been considered for the trajectory calculation, the same process is carried out in a tree-search algorithm, starting from the arrival body of each of the temporary sequences found so far. When the total mission duration reaches the maximum allowed time (i.e., 10 years in the current scenario) or no feasible solar-sail trajectories are found, the algorithm stops and the sequence is considered complete.

The computational time of the described sequence search increases as the number of feasible transfer trajectories increases due to the tree nature of the search itself. For this reason, the code has been implemented using mixed MATLAB/C code, speeding up the computations where bottlenecks have been found in the MATLAB code. Moreover, the algorithm is parallelized for different launch dates.

C. Local Pruning of the Database

A local pruning on the available NEA database is performed, based on astrodynamics: This has been carried out to work on a locally reduced database, for the reasons mentioned in Sec. III.B. As shown in Fig. 4, the local pruning is performed at each leg of the sequence and it depends on the starting body of the respective leg.

Four conditions for the local pruning of the database are taken into account: The first three criteria are related to the in-plane trajectory, whereas the fourth takes into account the orientation of the orbital planes:

1) The current spacecraft state is propagated in an outward and inward spiral by considering a control law that maximizes the semimajor axis change. The maximum and minimum semimajor axes obtained are then the maximum and minimum semimajor axes that the solar sail can reach starting from the current state and traveling for the maximum available time of flight. All NEAs with a semimajor axis outside the available range are therefore excluded from the locally pruned database for the current leg. To obtain the maximum and minimum semimajor axes, the locally optimal law for changing the semimajor axis through solar sailing, described in [28], is used.

2) As in the preceding case, the trajectory is propagated by considering a control law that maximizes the change of the eccentricity and thus a maximum range of possible eccentricity variation is found. Only those NEAs with eccentricity inside the available range are

Downloaded by UCHU KOKU KENKYU KAIHATSU KIKO on March 1, 2021 | http://arc.aiaa.org | DOI: 10.2514/1.G000470

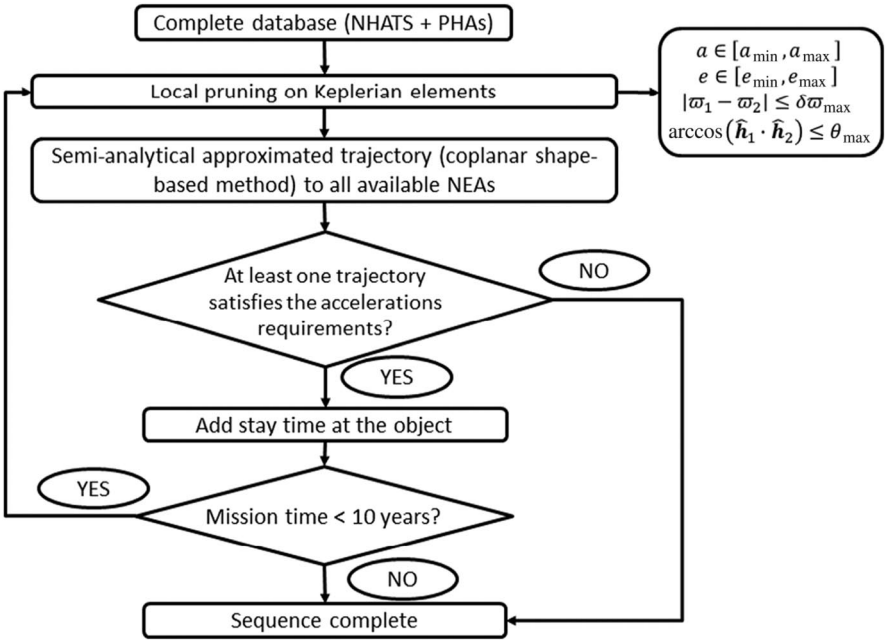

Fig. 4 Sequence search.

included in the locally pruned database for the current leg. The locally optimal law for changing the eccentricity through solar sailing, described in [28], is used for this second local pruning.

3) Defining the longitude of pericenter as $\varpi = \omega + \Omega$, a transfer trajectory between two orbits (subscripts 1 and 2) with a large $\delta\varpi = \text{mod}(\varpi_1 - \varpi_2, \pi)$ is more difficult to achieve as the eccentricities of the two orbits increase. For this reason, a threshold on the maximum variation of the longitude of pericenter has been considered for each object, taking into account the value of the eccentricity as follows:

$$\delta\varpi_{\max} := \pi(1-e)^2 \tag{9}$$

By using this threshold, the arrival object is removed from the locally pruned database if at least one of the following conditions is not satisfied:

$$\begin{cases} \text{mod}(\varpi_1 + \delta\varpi_{\max,1} + \pi, 2\pi) > \text{mod}(\varpi_2 - \delta\varpi_{\max,2} + \pi, 2\pi) \\ \text{mod}(\varpi_2 + \delta\varpi_{\max,2} + \pi, 2\pi) > \text{mod}(\varpi_1 - \delta\varpi_{\max,1} + \pi, 2\pi) \end{cases} \tag{10}$$

In Fig. 5, two examples (not to scale) are sketched to give a graphical view of the pruning on the longitude of pericenter given by Eq. (10). Figure 5a shows a case in which Eq. (10) is satisfied and, in fact, the ranges of possible variation of ϖ for the two objects overlap. On the other hand, in Fig. 5b, the orbit of the second object is more eccentric, so that the available range of variation of ϖ is smaller and does not overlap with the one of the first object. In this second case, the first condition in Eq. (10) is not satisfied and the second object is therefore not part of the locally pruned database for the current leg.

4) Let us define θ as the angle between the angular momenta of the two orbits:

$$\theta := \arccos(\hat{h}_1 \cdot \hat{h}_2) \tag{11}$$

Because a coplanar transfer is taken into account for the simplified trajectory description, a maximum value of θ is selected as the threshold to consider the second object to be part or not of the locally pruned database. This way, objects are not considered where a change of the inclination and/or the longitude of the ascending node would be too large in the three-dimensional case.

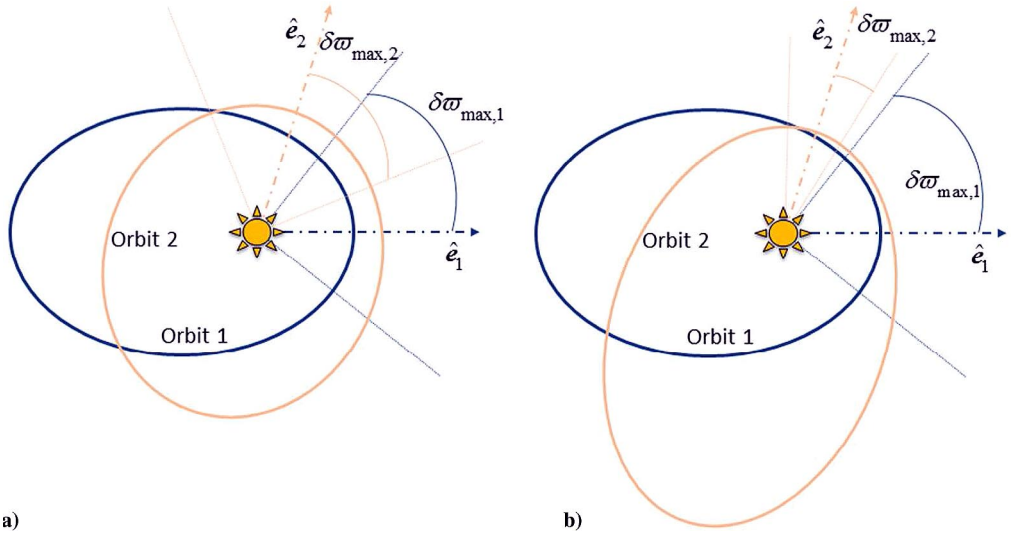

Fig. 5 Graphical view (not to scale) of pruning on longitude of pericenter: ranges of possible variation of longitude of pericenter for two objects a) overlap; b) do not overlap.

Downloaded by UCHU KOKU KENKYU KAIHATSU KIKO on March 1, 2021 | http://arc.aiaa.org | DOI: 10.2514/1.G000470

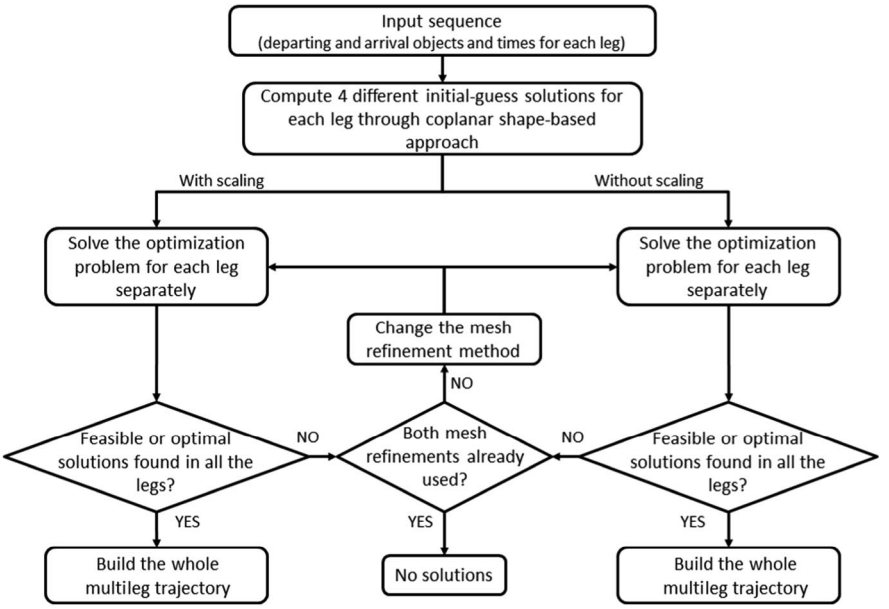

Fig. 6 Automatic optimization algorithm.

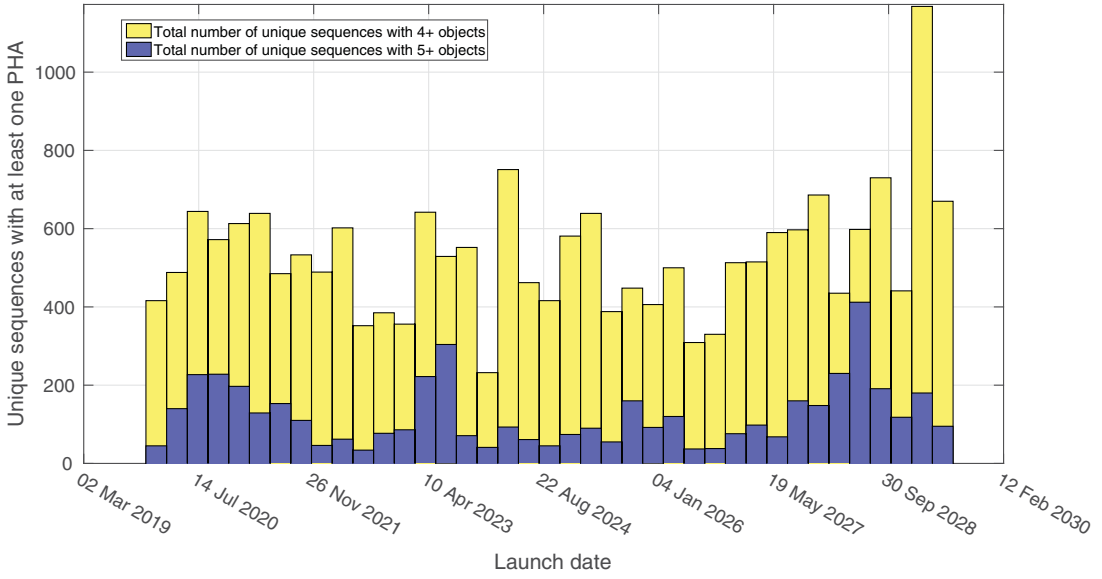

Fig. 7 Number of unique sequences with at least one PHA and four encounters as a function of the launch date.

IV. Sequence Optimization

Once complete sequences have been found, an optimization problem must be solved to find three-dimensional (3-D) solar-sail trajectories.

The equations of the dynamics are defined by the following set of ordinary differential equations of motion:

$$\dot{\boldsymbol{x}}(t) = \boldsymbol{A}(\boldsymbol{x})\boldsymbol{a} + \boldsymbol{b}(\boldsymbol{x}) \tag{12}$$

in which $\boldsymbol{A}(\boldsymbol{x})$ and $\boldsymbol{b}(\boldsymbol{x})$ are, respectively, the matrix and the vector of the dynamics as described in [29]. The propulsive acceleration $\boldsymbol{a}$ is given by Eq. (2).

The problem of finding the optimal control vector $\boldsymbol{u}^* = [N_r^* \quad N_\vartheta^* \quad N_h^*]^T$ such that the total mission duration is minimized, while fulfilling the dynamics constraints of Eq. (12) at any time, is solved via a direct transcription method [19]. The control vector $\boldsymbol{u}$ is bounded so that $N_\vartheta, N_h \in [-1, 1]$, whereas $N_r \in [0, 1]$ because of the inability of the solar sail to thrust toward the sun. The unit vector constraint is not explicitly enforced via a path constraint, but it is indirectly considered by normalizing all the components of the control vector with respect to its magnitude. In this way, there is one less constraint to be satisfied and the problem is numerically easier to solve. Note that the components of the sail normal unit vector are preferred to the sail cone and clock angles as control vector. Because of their periodicity, in fact, the sail control angles can lead to numerical issues within direct optimization methods.

The trajectory found through the coplanar shape-based approach is used as a first-guess solution for the optimizer, which transforms it into a complete 3-D trajectory. The optimizer used in this work is the general-purpose optimal control software GPOPS-II,[¶] which uses a variable-order adaptive Radau collocation method, together with sparse nonlinear programming (NLP). The NLP solver SNOPT [30]

[¶]Data available online at http://www.gpops2.com [retrieved 25 August 2015].

Downloaded by UCHU KOKU KENKYU KAIHATSU KIKO on March 1, 2021 | http://arc.aiaa.org | DOI: 10.2514/1.G000470

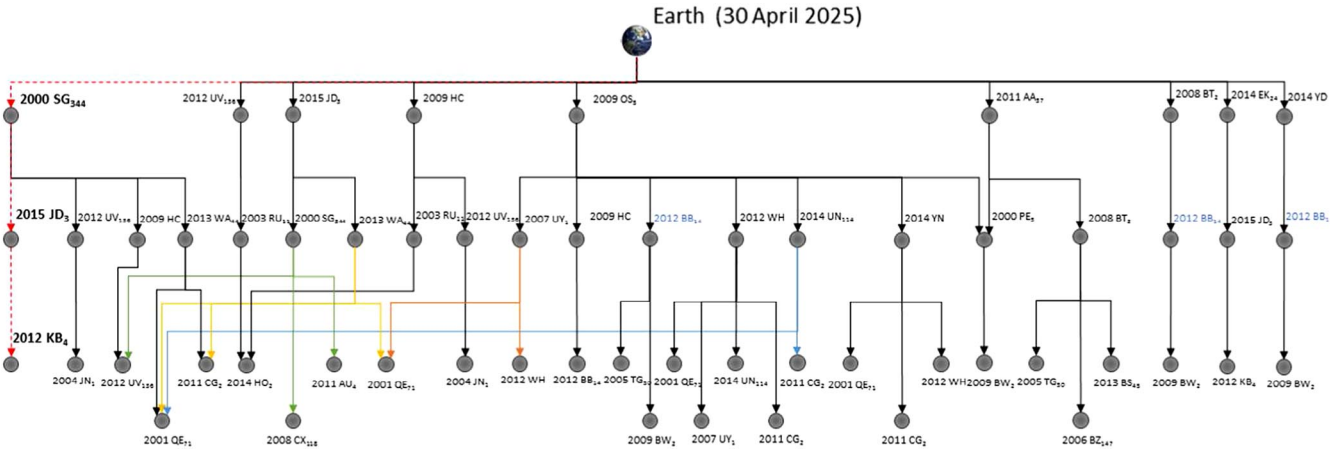

Fig. 8 Tree graph of first three legs of all sequences with five encounters found for launch date $t_0 = 30$ April 2025.

has been used within this study. Both the hp adaptive mesh refinement developed by Patterson et al. [18] and the one developed by Liu et al. [31] are considered for the optimization.

To help the numerical convergence of the optimizer, a scaled problem is taken into account for both the initial-guess generation and the actual optimization. A scaling used is so that $r_\oplus = 1$ and $\mu = 1$. By using this scaling and taking into account that the objects under study are NEAs, the magnitudes of position are always $\|\boldsymbol{r}\| = \mathcal{O}(1)$ and the characteristic acceleration $a_c = 0.2$ mm/s^2 of the solar sail becomes $a_c = 0.0337$ in normalized units. This scaling allows a description of the problem that is more suitable to numerical optimization, rather than using the international system units where $\|\boldsymbol{r}\|/a_c = \mathcal{O}(10^{15})$.

An algorithm has been developed in MATLAB to find the optimal trajectory in terms of total mission duration (Fig. 6). Given the selected sequence, the algorithm performs as follows:

1) The algorithm automatically computes the initial guess for each leg separately by means of the shape-based approach with the objective function of Eq. (6), as described in Sec. II.B. To avoid possible numerical problems in the optimization phase that can affect the convergence of the optimizer, several initial-guess solutions are generated for each leg. That is, the trajectory is propagated by considering both a constant control law between two points of the shaped function and a spline interpolation of the control law. Moreover, two different stopping criteria are taken into account in the GA, so that four different initial-guess solutions are generated for each leg.

2) The algorithm optimizes the 3-D trajectory leg by leg. Each initial guess is optimized both without considering any further scaling method and by further scaling the problem through the "automatic-guessUpdate" choice provided by GPOPS-II. Moreover, if no feasible or optimal solutions are found for the current leg, the default hp adaptive mesh refinement is changed so that the one developed by Liu et al. [31] is used for the whole optimization. Within this optimization phase, the solution of each leg is constrained to start at least 2 days after the arrival of the previous leg. In this way, a multiphase optimization, which would only be used to reduce the total mission duration, is not necessary.

3) Finally, if at least one feasible solution is found in all the legs individually, the whole multileg trajectory is built.

V. Multiple-Asteroids Rendezvous Mission Design

The methodology proposed has been applied considering a sailcraft with a characteristic acceleration $a_c = 0.2$ mm/s^2. In the following subsections, the results of the sequence search and a fully optimized sequence are shown.

A. Sequence Search Results

Starting from the launch date $t_0 = 28$ November 2019, a systematic search of sequences has been carried out on a set of launch dates spanning about 10 years with a step size of three months ($t_0 \in$ [28 November 2019, 06 October 2029]). This choice of launch dates allows short- and long-term variations in the phasing between objects to be taken into account. A stay time of 100 days has been considered between two consecutive legs within the sequence-search algorithm (Fig. 4).

This search resulted in more than 4800 unique sequences made of five encounters, of which at least one is a PHA. Moreover, many more sequences have been found by using this approach as compared with a previous study [32]. This is mainly due to the different pruning criteria used for the eccentricity and the inclination. Regarding the latter, sequences with highly inclined objects have been discarded in [32] because of the 5 deg threshold on the inclination taken into account to consider the transfers as planar. On the other hand, this paper shows the possibility of finding sequences containing asteroids with inclination higher than 5 deg (e.g., the fully optimized sequence described in Sec. V.B).

Figure 7 shows the number of unique sequences found for each launch date. Only those sequences with at least one PHA and at least four encounters are taken into account for the plot. Here, the term unique sequence refers to the sequence of objects only, without

Table 4 Properties of encounters of considered sequence

Object	2000 SG_{344}	2015 JD_3	2012 KB_4	2008 EV_5	2014 MP
Orbital type	Aten	Amor	Amor	Aten	Amor
Semimajor axis, AU	0.977	1.058	1.093	0.958	1.050
Eccentricity	0.067	0.009	0.061	0.083	0.029
Inclination, deg	0.111	2.730	6.328	7.437	9.563
Absolute magnitude	24.7	25.6	25.3	20	26
Estimated size, m	35–75	20–50	20–50	260–590	17–37
EMOID, AU	0.0008	0.054	0.073	0.014	0.020
PHA	No	No	No	Yes	No
NHATS	Yes	Yes	Yes	Yes	Yes

Downloaded by UCHU KOKU KENKYU KAIHATSU KIKO on March 1, 2021 | http://arc.aiaa.org | DOI: 10.2514/1.G000470

Object	Stay time, days	Start	End	Time of flight, days
Earth	—	10 May 2025 (30 April 2025)	26 Feb. 2027 (11 March 2027)	657 (680)
2000 SG_{344}	123 (100)	29 June 2027 (19 June 2027)	06 Sept. 2028 (31 Oct. 2028)	436 (500)
2015 JD_3	164 (100)	18 Feb. 2029 (08 Feb. 2029)	24 Sept. 2030 (14 Nov. 2030)	584 (644)
2012 KB_4	160 (100)	04 March 2031 (22 Feb. 2031)	29 Sept. 2032 (30 Nov. 2032)	576 (647)
2008 EV_5	171 (100)	20 March 2033 (10 March 2033)	30 Sept. 2034 (25 Nov. 2034)	560 (625)
2014 MP	—			

Fig. 9 Mission parameters for the considered sequence (values in brackets are the ones found through the sequence-search algorithm and used as initial guess for the optimizer).

Downloaded by UCHU KOKU KENKYU KAIHATSU KIKO on March 1, 2021 | http://arc.aiaa.org | DOI: 10.2514/1.G000470

taking into account the possible differences in time. It is important to note that more than 400 unique sequences with five encounters and at least one PHA have been found for a single launch date ($t_0 = 14$ April 2028). This number increases up to more than 1000 if the sequences with more than four encounters are taken into account (for $t_0 = 09$ January 2029).

Figure 8 shows an example of the first three legs of all the sequences with five encounters and at least a PHA found for the launch date $t_0 = 30$ April 2025. The graph shows the typical tree nature of the solution. Two different sequences are considered having a rendezvous with the same object when the arrival times differ by 40 days at most. For example, the object 2012 BB_4 appears three times in the second leg, but the rendezvous times differ by more than 100 days. Therefore, these are considered as three separate branches of the solution tree. The sequence characterized by the dashed line is the fully optimized one shown in Sec. V.B.

Figure 8 shows how several sequences are partly repeated. This allows the target asteroids to be easily changed, even after launch, if

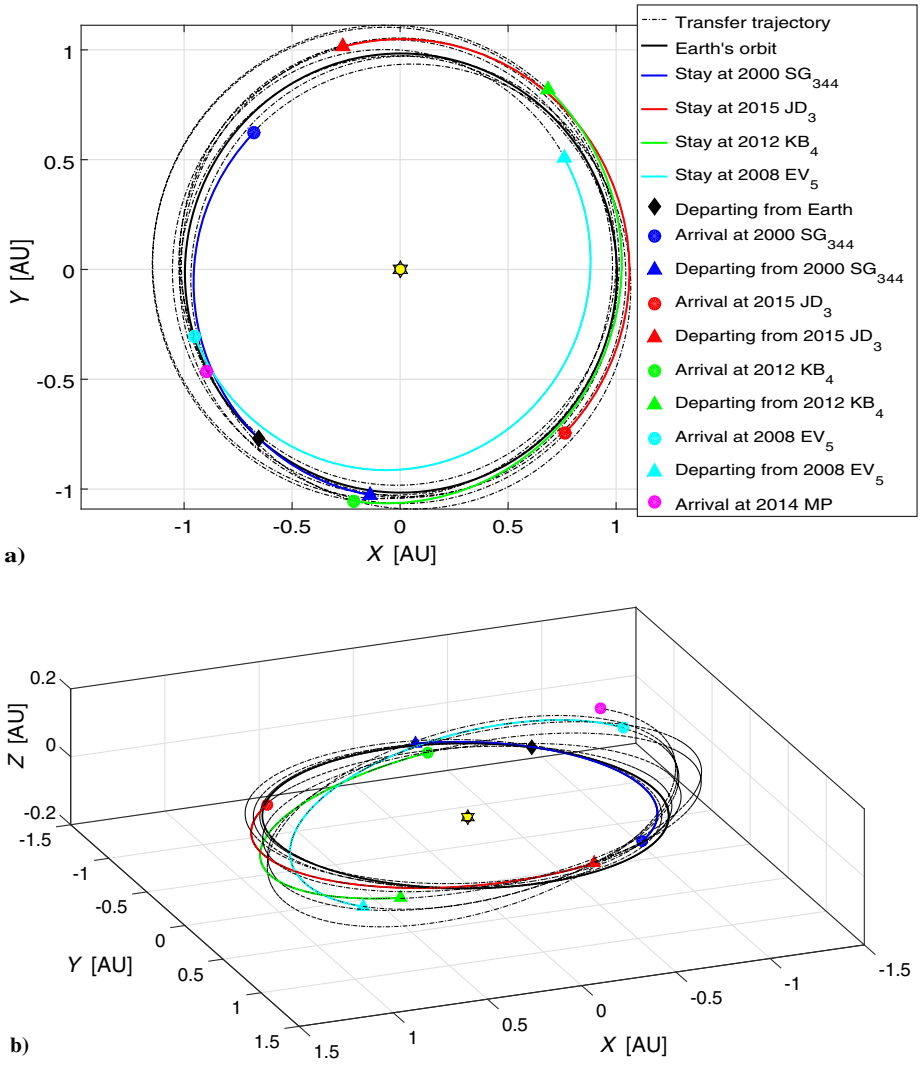

Fig. 10 Heliocentric view of complete three-dimensional trajectory of considered sequence: a) ecliptic plane view; b) 3-D view.

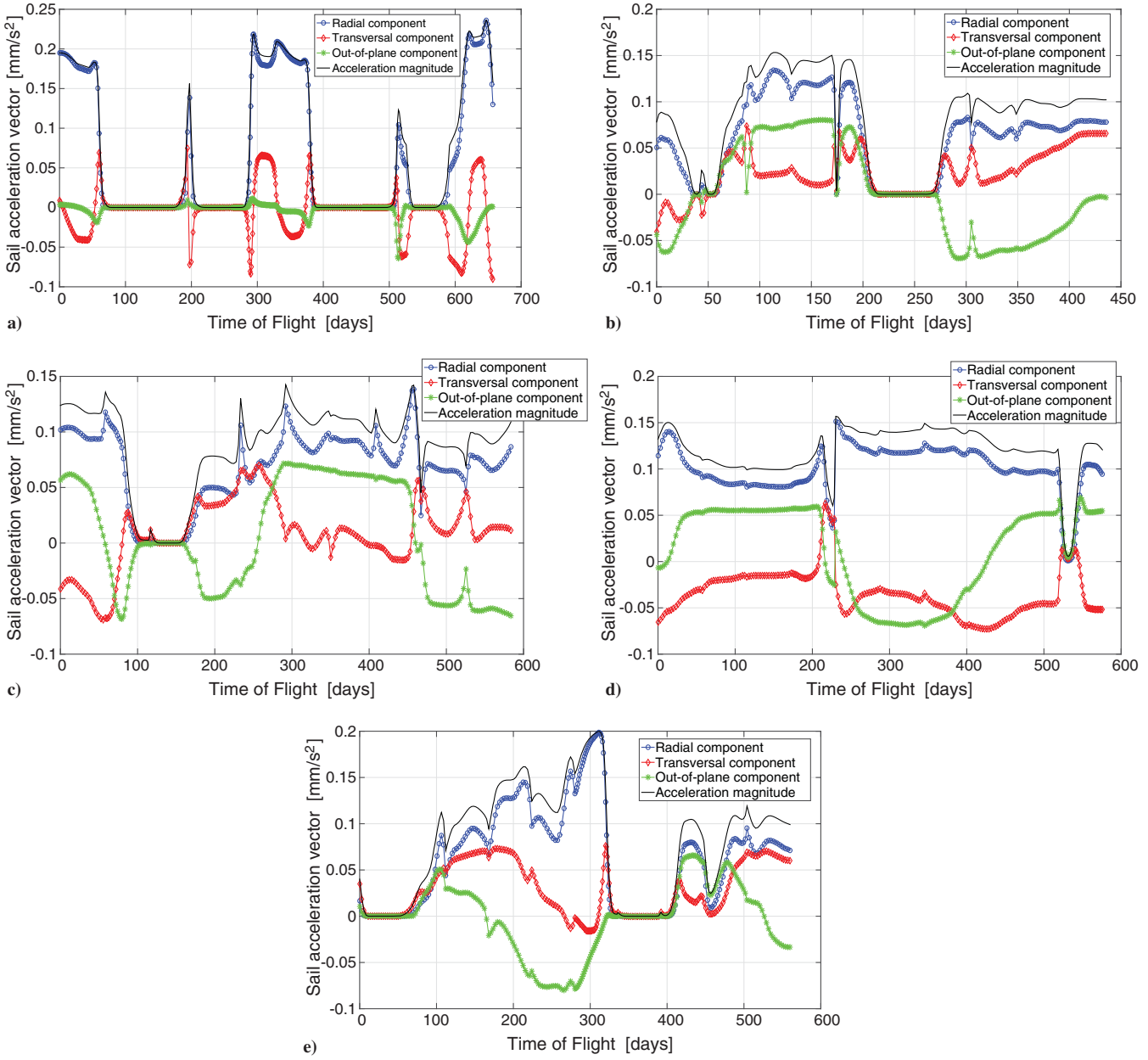

Fig. 11 Acceleration components history on each transfer leg.

needed. Moreover, because of the propellantless nature of the solar-sail technology, such a change is theoretically easier with a solar sail than with an electrical propulsion system.

Because of the tree nature of the sequence search and the need of a genetic algorithm run to check the existence of each trajectory, the whole search has been carried out by running several parallel searches for the 41 launch dates over three different machines: a 3.4 GHz Core i7-3770, a 3.4 GHz Core i7-4770, and a 2.3 GHz Core AMD Opteron 6376. The first two machines have 16 GB of RAM and run Windows 7. The third one is part of the University of Glasgow Computer Cluster Facility,[***] has up to 8 GB of RAM per core, and runs CentOS 6. Considering only those simulations carried out on the latter, which is the slowest machine, the average computational time for each sequence-search run is about 41.3 days, where each successful run of the shape-based approach took about 60 s on average.

B. Sequence Optimization Results

One sequence has been selected, and fully optimized by means of the automatic algorithm described in Sec. IV, to validate the proposed methodology. This sequence has been selected among all the sequences found with five encounters, of which one is a PHA. All the objects in the selected sequence are part of the NHATS database taken into account and the fourth one, 2008 EV_5, is also classified as a PHA. Table 4 shows the encountered bodies in the sequence. The estimated size of the objects are calculated from the Minor Planet Center table of conversion from absolute magnitude to diameter, taking into account an albedo in the range 0.05–0.25.[†††]

Note that, in Table 4, the change in inclination between two consecutive objects is always less than 5 deg, which is the threshold used for the coplanar approximation [Eq. (11)]. However, Table 4 shows that the inclination of the encounters increases by moving from an object to the following, eventually reaching an inclination of about 10 deg for the last encounter. This result is significantly

***Data available online at http://www.gla.ac.uk/services/it/hpcc/ [retrieved 24 August 2015].

†††Data available online at http://www.minorplanetcenter.net/iau/lists/Sizes.html [retrieved 25 August 2015].

Downloaded by UCHU KOKU KENKYU KAIHATSU KIKO on March 1, 2021 | http://arc.aiaa.org | DOI: 10.2514/1.G000470

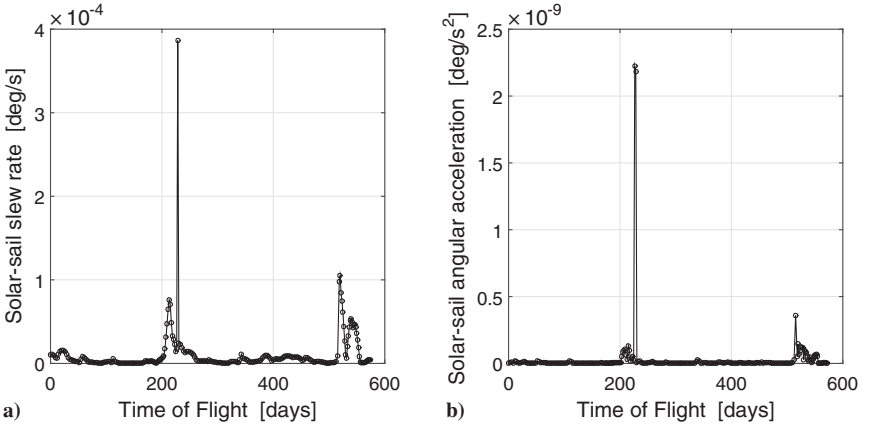

Fig. 12 Sail slew rate a) and sail angular acceleration b) over time on the fourth leg.

Downloaded by UCHU KOKU KENKYU KAIHATSU KIKO on March 1, 2021 | http://arc.aiaa.org | DOI: 10.2514/1.G000470

different with respect to what could be found by following the method described in [32], in which a threshold of 5 deg on the maximum inclination was considered within the pruning of the whole database. Therefore, this particular sequence could not have been found because the last three asteroids have an inclination larger than the 5 deg threshold.

By following the optimization steps described in Sec. IV, a multiphase solution was found. The characteristics of the mission are briefly described in Fig. 9. The values in brackets are the ones found through the sequence-search algorithm and used as initial guess for the optimizer. Note that the stay time in brackets is always equal to 100 days, because it is a value decided a priori, as specified in Sec. V. A. The end-to-end optimization phase, as described in Sec. IV, needed about 3 h of computational time. It is important to note, however, that this is the overall time required by the automated algorithm and it also takes into account the time spent within the optimizer when the convergence was not achieved. If only the time spent by the optimizer to find the shown trajectory is considered, a total time of 330 s is needed for the end-to-end optimization of the whole multileg trajectory.

The sail is injected directly into an interplanetary trajectory at Earth, with zero hyperbolic excess energy. The mission is completed in about 9.4 years after departing from Earth on 10 May 2025. It is worth noting that the sail spends at least four months in the proximity of each object, giving sufficient time for close-up NEA observations.

The two-dimensional projection of the complete trajectory of the considered sequence is shown in Fig. 10. The stay times at the objects are highlighted against the whole trajectory. The orbit of the Earth is plotted as well. Plots of the control histories on each leg are plotted in Fig. 11. The three components of the acceleration vector in the orbital reference frame over time are shown, together with the magnitude of the acceleration over time.

It is worth noting that, despite the few spikes in the control history shown in the plots in Fig. 11, the results are feasible by a solar sail with the currently available technology. This can be demonstrated by studying both slew rate and angular acceleration of the sail required to follow the control histories shown in Fig. 11. Denoting the angle ζ as the angle between two consecutive attitudes [i.e., $\cos(\zeta) = \hat{\boldsymbol{N}}(t_i) \cdot \hat{\boldsymbol{N}}(t_{i+1})$], the sail slew rate $\dot{\zeta}$ is defined as the rate of change of the sail attitude. Figure 12a shows the sail slew rate for leg 4 of the current five-NEA sequence. This leg has been chosen because it is the one with the highest value of slew rate. Figure 12a shows that the sail slew rate is always $\dot{\zeta} < 4 \times 10^{-4}$ deg /s. Studies on solar-sail attitude control in the literature show that a solar sail with a characteristic acceleration of $a_c \simeq 0.1$ mm/s^2 is able to perform a 35 deg maneuver in less than 3 h [4,33], thus with an average sail slew rate of $\dot{\zeta} \simeq 5 \times 10^{-3}$ deg /s. Moreover, Wie and Murphy [33] show that the spike in the slew rate for a 35 deg yaw maneuver is $\dot{\zeta}_{\max} \simeq 0.03$ deg /s, which is higher than the maximum slew rate required during the whole mission described here.

However, the angular acceleration needed to follow the control found through the optimization algorithm shall also be investigated to verify the feasibility of such a mission from the attitude-control point of view. Figure 12b shows the angular acceleration for the fourth transfer leg of the considered sequence, obtained by time differentiation of the sail slew rate shown in Fig. 12a. It is possible to see a spike in the angular acceleration, related to the pick in the slew rate, of $\ddot{\zeta} \simeq 2.2 \times 10^{-9}$ deg /s^2. For comparison, note that the maximum torque allowed for a Mars rendezvous mission in [34] (pp. 69–86) is set to $\tau_{\max} = 10^{-3}$ Nm. Because a solar sail with an area $A = (160\text{ m})^2$ and a total mass $m = 450$ kg is taken into account [34], the equivalent maximum allowed angular acceleration is $\ddot{\zeta}_{\max} \simeq 6 \times 10^{-8}$ deg /s^2, considering a perfect square sail rotating around one of the principal axes of inertia on the sail plane. This value is larger than the largest one needed to achieve the proposed transfers.

Because no explicit constraints have been set on either the sail slew rate or the angular acceleration within the optimization algorithm, further optimization may be needed if stricter constraints are required.

VI. Conclusions

A methodology to find sequences of encounters for multiple NEA rendezvous missions through solar sailing was presented. To increase the possibility of finding objects of sufficient interest for planetary defense, science, and technology demonstration, only potentially hazardous asteroids (PHAs) and Near-Earth Object Human Space Flight Accessible Target Study (NHATS) asteroids were preselected for being part of the database in this study. In addition to selecting the objects of interest, this allowed a reduction in the total computational effort needed for finding trajectory sequences. A search-and-prune algorithm was used to find sequences of encounters for a multiple-NEA rendezvous mission. Local pruning, based on astrodynamics, was used to find as many sequences as possible within an acceptable amount of computational time. Therefore, a shape-based trajectory model for solar sailing was developed to have a good approximation of the trajectory, ensuring that the sequence is likely to be feasible with a detailed trajectory model. Finally, an automatic algorithm was developed to optimize the full solar-sail trajectory of the sequences chosen from the output of the sequence search.

A wide range of launch dates were tested. This was done to have more flexibility on the initial mission time and the possibility to choose a launch window also on the basis of the amount of possible sequences. This work resulted in more than 4800 unique sequences made of four NHATS asteroids and at least one PHA within less than 10 years of total mission duration. Among all of those sequences, one was selected to be shown and fully optimized for the complete

multileg trajectory. This resulted in a total mission duration of less than 10 years and at least four months spent in the vicinity of each object for close-up observations.

Finally, the novel coplanar shape-based approach for solar sailing has been demonstrated to give good results both within the sequence search and as an initial-guess solution for the three-dimensional direct optimization.

Appendix: Supplementary Data

Supplementary data associated with this article can be found at http://dx.doi.org/10.5525/gla.researchdata.326. The data set contains the names and ephemerides of the objects part of the reduced database discussed in Sec. III.A and the data of the full trajectory shown.

Acknowledgments

Alessandro Peloni gratefully acknowledges support for this research from the School of Engineering at the University of Glasgow and the Engineering and Physical Sciences Research Council for funding his research under the James Watt sponsorship program. The authors thank Anil Rao and Mark Meenan for their precious support given with GPOPS-II and the University of Glasgow Computer Cluster Facility, respectively.

References

[1] Dachwald, B., and Seboldt, W., "Multiple Near-Earth Asteroid Rendezvous and Sample Return Using First Generation Solar Sailcraft," *Acta Astronautica*, Vol. 57, No. 11, 2005, pp. 864–875. doi:10.2514/1.6797

[2] Ceriotti, M., and McInnes, C. R., "Generation of Optimal Trajectories for Earth Hybrid Pole Sitters," *Journal of Guidance, Control, and Dynamics*, Vol. 34, No. 3, 2011, pp. 847–859. doi:10.2514/1.50935

[3] Circi, C., "Simple Strategy for Geostationary Stationkeeping Maneuvers Using Solar Sail," *Recent Patents on Space Technology*, Vol. 28, No. 2, 2005, pp. 249–253. doi:10.2514/1.6797

[4] Peloni, A., Barbera, D., Laurenzi, S., and Circi, C., "Dynamic and Structural Performances of a New Sailcraft Concept for Interplanetary Missions," *Scientific World Journal*, Vol. 2015, 2015, Paper 714371. doi:10.1155/2015/714371

[5] Grundmann, J.-T., et al., "From Sail to Soil—Getting Sailcraft Out of the Harbour on a Visit to One of Earth's Nearest Neighbours," *Fourth IAA Planetary Defense Conference — PDC 2015*, International Academy of Astronautics Paper IAA-PDC-15-04-17, 2015.

[6] Alemany, K., and Braun, R. D., "Survey of Global Optimization Methods for Low-Thrust, Multiple Asteroid Tour Missions," *AAS/AIAA Space Flight Mechanics Meeting*, American Astronautical Soc. Paper 07-211, 2007.

[7] Li, S., Zhu, Y., and Wang, Y., "Rapid Design and Optimization of Low-Thrust Rendezvous/Interception Trajectory for Asteroid Deflection Missions," *Advances in Space Research*, Vol. 53, No. 4, 2014, pp. 696–707. doi:10.1016/j.asr.2013.12.012

[8] Taheri, E., and Abdelkhalik, O., "Shape Based Approximation of Constrained Low-Thrust Space Trajectories Using Fourier Series," *Journal of Spacecraft and Rockets*, Vol. 49, No. 3, 2012, pp. 535–546. doi:10.2514/1.58789

[9] Novak, D. M., and Vasile, M., "Improved Shaping Approach to the Preliminary Design of Low-Thrust Trajectories," *Journal of Guidance, Control, and Dynamics*, Vol. 34, No. 1, 2011, pp. 128–147. doi:10.2514/1.50434

[10] Sims, J. A., Finlayson, P. A., Rinderle, E. A., Vavrina, M. A., and Kowalkowski, T. D., "Implementation of a Low-Thrust Trajectory Optimization Algorithm for Preliminary Design," *AIAA/AAS Astrodynamics Specialist Conference*, American Institute of Aeronautics and Astronautics Paper 2006-6746, 2006.

[11] Zuiani, F., Vasile, M., Palmas, A., and Avanzini, G., "Direct Transcription of Low-Thrust Trajectories with Finite Trajectory Elements," *Acta Astronautica*, Vol. 72, 2012, pp. 108–120. doi:10.1016/j.actaastro.2011.09.011

[12] Izzo, D., "Lambert's Problem for Exponential Sinusoids," *Journal of Guidance, Control, and Dynamics*, Vol. 29, No. 5, 2006, pp. 1242–1245. doi:10.2514/1.21796

[13] Petropoulos, A. E., and Longuski, J. M., "Shape-Based Algorithm for the Automated Design of Low-Thrust, Gravity Assist Trajectories," *Journal of Spacecraft and Rockets*, Vol. 41, No. 5, 2004, pp. 787–796. doi:10.2514/1.13095

[14] Dachwald, B., et al., "Gossamer Roadmap Technology Reference Study for a Multiple NEO Rendezvous Mission," *Advances in Solar Sailing*, edited by Macdonald, M., Springer Praxis Books, Springer–Verlag, Berlin, 2014, pp. 211–226.

[15] Bando, M., and Yamakawa, H., "Near-Earth Asteroid Flyby Survey Mission Using Solar Sailing Technology," *Journal of Astronautical Sciences*, Vol. 58, No. 4, 2011, pp. 569–581. doi:10.1007/bf03321532

[16] McInnes, C. R., "Inverse Solar Sail Trajectory Problem," *Journal of Guidance, Control, and Dynamics*, Vol. 26, No. 2, 2003, pp. 369–371. doi:10.2514/2.5057

[17] Garg, D., Patterson, M. A., Francolin, C., Darby, C. L., Huntington, G. T., Hager, W. W., and Rao, A. V., "Direct Trajectory Optimization and Costate Estimation of Finite-Horizon and Infinite-Horizon Optimal Control Problems Using a Radau Pseudospectral Method," *Computational Optimization and Applications*, Vol. 49, No. 2, 2011, pp. 335–358. doi:10.1007/s10589-009-9291-0

[18] Patterson, M. A., Hager, W. W., and Rao, A. V., "A ph Mesh Refinement Method for Optimal Control," *Optimal Control Applications and Methods*, Vol. 36, No. 4, 2014, pp. 398–421. doi:10.1002/oca.2114

[19] Patterson, M. A., and Rao, A. V., "GPOPS–II: A MATLAB Software for Solving Multiple-Phase Optimal Control Problems Using hp–Adaptive Gaussian Quadrature Collocation Methods and Sparse Nonlinear Programming," *ACM Transactions on Mathematical Software*, Vol. 41, No. 1, 2014, Paper 1. doi:10.1145/2558904

[20] Betts, J. T., "Survey of Numerical Methods for Trajectory Optimization," *Journal of Guidance, Control, and Dynamics*, Vol. 21, No. 2, 1998, pp. 193–207. doi:10.2514/2.4231

[21] Wall, B. J., and Conway, B. A., "Shape-Based Approach to Low-Thrust Rendezvous Trajectory Design," *Journal of Guidance, Control, and Dynamics*, Vol. 32, No. 1, 2009, pp. 95–102. doi:10.2514/1.36848

[22] Novak, D. M., "Methods and Tools for Preliminary Low Thrust Mission Analysis," Ph.D. Dissertation, School of Engineering, Univ. of Glasgow, Glasgow, Scotland, U.K., 2012.

[23] De Pascale, P., and Vasile, M., "Preliminary Design of Low-Thrust Multiple Gravity-Assist Trajectories," *Journal of Spacecraft and Rockets*, Vol. 43, No. 5, 2006, pp. 1065–1076. doi:10.2514/1.19646

[24] Walker, M. J. H., Ireland, B., and Owens, J., "A Set Modified Equinoctial Orbit Elements," *Celestial Mechanics*, Vol. 36, No. 4, 1985, pp. 409–419. doi:10.1007/bf01227493

[25] *MATLAB User's Guide*, Ver. R2014b, MathWorks, Natick, MA, 2014.

[26] Mengali, G., and Quarta, A. A., "Solar Sail Trajectories with Piecewise-Constant Steering Laws," *Aerospace Science and Technology*, Vol. 13, No. 8, 2009, pp. 431–441. doi:10.1016/j.ast.2009.06.007

[27] Barbee, B. W., Esposito, T., Pinon, E., Hur-Diaz, S., Mink, R. G., and Adamo, D. R., "A Comprehensive Ongoing Survey of the Near-Earth Asteroid Population for Human Mission Accessibility," *AIAA Guidance, Navigation, and Control Conference*, AIAA Paper 2010-8368, 2010.

[28] McInnes, C. R., *Solar Sailing: Technology, Dynamics and Mission Applications*, Springer Praxis, Chichester, England, U.K., 1999, pp. 136–143.

[29] Betts, J. T., *Practical Methods for Optimal Control and Estimation Using Nonlinear Programming*, Soc. for Industrial and Applied Mathematics, Philadelphia, PA, 2010, pp. 265–267.

[30] Gill, P., Murray, W., and Saunders, M., "SNOPT: An SQP Algorithm for Large-Scale Constrained Optimization," *SIAM Review*, Vol. 47, No. 1, 2005, pp. 99–131. doi:10.1137/S0036144504446096

[31] Liu, F., Hager, W. W., and Rao, A. V., "Adaptive Mesh Refinement Method for Optimal Control Using Nonsmoothness Detection and Mesh Size Reduction," *Journal of the Franklin Institute*, Vol. 352, No. 10, 2015, pp. 4081–4106. doi:10.1016/j.jfranklin.2015.05.028

Downloaded by UCHU KOKU KENKYU KAIHATSU KIKO on March 1, 2021 | http://arc.aiaa.org | DOI: 10.2514/1.G000470

[32] Peloni, A., Ceriotti, M., and Dachwald, B., "Preliminary Trajectory Design of a Multiple NEO Rendezvous Mission Through Solar Sailing," *65th International Astronautical Congress*, International Astronautical Federation Paper IAC-14-C1.9.7, 2014.

[33] Wie, B., and Murphy, D., "Solar-Sail Attitude Control Design for a Sail Flight Validation Mission," *Journal of Spacecraft and Rockets*, Vol. 44, No. 4, 2007, pp. 809–821. doi:10.2514/1.22996

[34] Borggräfe, A., "Analysis of Interplanetary Solar Sail Trajectories with Attitude Dynamics," Diploma Thesis, Inst. of Flight System Dynamics, RWTH Aachen University, Aachen, Germany, 2011.

Downloaded by UCHU KOKU KENKYU KAIHATSU KIKO on March 1, 2021 | http://arc.aiaa.org | DOI: 10.2514/1.G000470